Proc. of the 5th WSEAS/IASME Int. Conf. on Electric Power Systems, High Voltages, Electric Machines, Tenerife, Spain, December 16-18, 2005 (pp74-79)

Control of Synchronous Motors using the Causal Ordering Graph, Part II: Control Design

Ghislain REMY, Pierre-Jean BARRE, Jean-Paul HAUTIER
Laboratory of Power Electronics and Electrical Engineering of Lille (L2EP)
Technological Research Team – ERT CEMODYNE
ENSAM, 8 Bd Louis XIV, 59046 Lille Cedex
FRANCE
barre@lille.ensam.fr http://www.lille.ensam.fr/cemodyne

Abstract: - In Part I, we have presented models of rotary and linear permanent magnet synchronous motors by using the Causal Ordering Graph (COG). This paper presents different control strategies deduced from established models with the inversion principle of the COG. Control strategies are developed in Concordia's reference frame (α-β) and Park's reference frame (d-q). Then, principles of controller design are laid out for each selected control strategy. Next, several propositions are made about estimator and anticipation structure. Finally, experimental results validating the effectiveness of our purpose on a permanent magnet linear synchronous motor are presented.

Key-Words: - Causal Ordering Graph, Linear Synchronous Motor, Control Strategy, Controller Design.

1 Introduction

Electrical drive controls are the focus of numerous articles, and bibliography is particularly vast on this subject. It isn't in our purpose to provide a complete analysis of all the existing control strategy. But it's enlightening to make a brief review of the most important control strategies.

1.1 Control strategy of synchronous motors

It is generally agreed that torque control strategies for alternative machines can be classified in three classes:

The first is based on steady-state considerations and classified under the name of scalar control strategies. These techniques generate references from average or impulse values. The main implicit assumption is to consider that the electromechanical mode prevails [1]. These laws are considered as static control laws, and are sufficient in variable speed applications, where inertial charges are sufficient, or with low dynamic systems. A main drawback of this solution is noticeable at low speeds with a very hard control: in fact, where the modes of the mechanical parts are too close to the electrical one.

A second class is named flux-oriented vector control and emerged from the choice to hold the instant torque close to its average value, whatever the working point and its evolution speed might be. These laws are built on dynamical models of studied machines [2], [3]. In order to reduce the complexity and to offer an easier control strategy, as for a DC motor, models are designed in Park's reference frame, a so-called synchronous reference frame (d-q). Indeed, in Park's reference frame, which is fixed to the rotating field, all the variables being considered are constant at a steady speed. These quantities can be regard as the useful parts of alternative values, which are only carrier signals for the controllers.

The Direct Torque Control makes up the third class. This solution is linked to the choice of the inverter which feeds the machine [4]. The aim is to keep both the flux and the torque close to their reference values by changing the supply vector at each instant. Furthermore, depending of the number of voltage levels given by the inverter, the precision of the correction will change [5]. This simple solution involves compromises between precision and the commutation frequency of the semi-conductors.

In this paper, by applying the inverse principle of the Causal Ordering Graph (COG), we propose different vector control structures. The controllers in the diphase (α-β) stationary reference frame are designed with multiple frequency resonant controllers. Then, we propose a controller design in the synchronous (d-q) reference frame with IP controllers. Several propositions are made about estimator and anticipation structure. As shown in Part I, rotary and linear synchronous motors can be modelled in the same way. So we have chosen a permanent magnet linear synchronous motor (PMLSM) to validate the effectiveness of our methods.

1.2 Inversion Principle of COG

The process models defined in Part I are now used to deduce the control structure by using the inversion principle of the COG, which is defined as follows [6]:

Rigid processors can be directly inverted:

$$\begin{aligned} &R \to y = R(u), \quad R_c \to u_{reg} = C(y_{ref}) \\ &IF \quad u = u_{reg} \text{ AND } C = R^{-1}, \text{ THEN } y = y_{ref} \end{aligned} \tag{1}$$

Causal processors call for an indirect inversion (closed control loop):

$$\begin{aligned} &R \to y = R(u), \quad R_c \to u_{reg} = C(y_{ref} - \hat{y}) \\ &IF \quad u = u_{reg} \text{ AND } C \to \infty, \text{ THEN } y \to y_{ref} \end{aligned} \tag{2}$$

The causal and rigid inversions are presented in Fig.1:

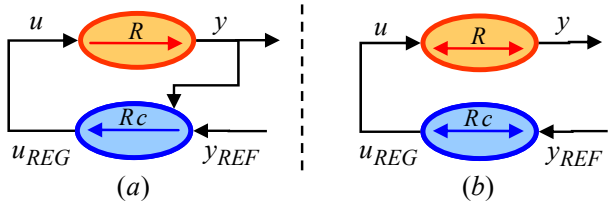

Fig.1: Inversion Principle of the COG:
(a) causal relation, (b) rigid relation.

2 Thrust Control Structure

2.1 Control structure in (*α-β*) reference frame

If we apply the inversion principle on our PMLSM model, we obtain the controller design depicted in Fig.2:

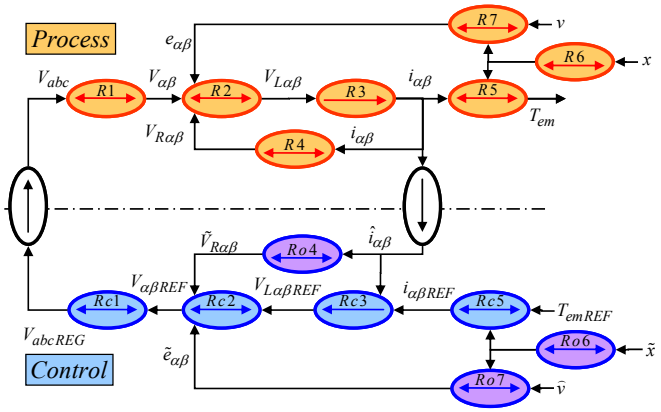

Fig.2: PMLSM thrust control scheme in (*α-β*)

The different relations are given by:

$$Rc2 \rightarrow V_{\alpha\beta REF} = V_{L\alpha\beta REF} - \tilde{e}_{\alpha\beta} - \tilde{V}_{R\alpha\beta}$$

$$Rc3 \rightarrow V_{L\alpha REF} = C_\alpha (i_{\alpha ref} - \hat{i}_\alpha)$$

$$Ro4 \rightarrow \tilde{V}_{R\alpha\beta} = \tilde{R}_{\alpha\beta} \cdot \hat{i}_{\alpha\beta}$$

$$Rc5 \rightarrow \begin{cases} i_{\alpha REF} = \dfrac{-T_{emREF} \cdot \sin(\hat{\theta}_e)}{\sqrt{3/2} \cdot N_p \cdot \hat{\phi}_f} \\ i_{\beta REF} = \dfrac{T_{emREF} \cdot \cos(\hat{\theta}_e)}{\sqrt{3/2} \cdot N_p \cdot \hat{\phi}_f} \end{cases}$$

$$Ro6 \rightarrow \begin{cases} \dfrac{d\tilde{\phi}_\alpha}{dx} = -\sqrt{\dfrac{3}{2}} N_p . \hat{\phi}_f \cdot \sin(\hat{\theta}_e) \\ \dfrac{d\tilde{\phi}_\beta}{dx} = \sqrt{\dfrac{3}{2}} N_p . \hat{\phi}_f \cdot \cos(\hat{\theta}_e) \end{cases}$$

$$Ro7 \rightarrow \tilde{e}_{\alpha\beta} = \hat{v} \cdot \frac{d\tilde{\phi}_{\alpha\beta}}{dx}$$

The *Ro*4 processor is defined to compensate the resistor voltage. In order to have perfectly realised compensation, the resistance value has to be well identified. With a varying resistor value, this estimator could be incremented, for example, with a thermal model of the resistor. But the *R*o4 processor will stay the same; it's an estimator of the resistor voltage. Thus, the scheme remains intuitively readable.

The *Rc*3 processor contains the controller, which has to reduce the error between the reference currents and the measured currents.

The *Rc*5 and *Ro*7 processors are not directly in the current loop, which is represented with the *R*1, *R*2, *R*3, *Rc*3, *Rc*2 and *Rc*1 processors. So the *Rc*5 processor represents the estimation of the nonlinear rigid processor *R*5, and is needed to deliver the reference currents. The *Ro*7 represents the estimation of the back-EMF, and is needed to compensate the influences of voltages induced by movement.

In the *Rc*5 processor, there are four inputs: i_α, i_β, $d\Phi_\alpha/dx$ and $d\Phi_\beta/dx$. But there is only one output: the thrust T_{em}. We estimate $d\Phi_\alpha/dx$ and $d\Phi_\beta/dx$ in the *Ro*6 processor. The *Rc*5 processor is called a strategy block, because we have several choices to generate the reference currents. Here, we have opted for the optimal reference currents to produce required thrust without ripples forces. Furthermore, reduction of ohmic losses induced by harmonics currents should be interesting [7]. Obviously, to maximize the efficiency, the current harmonics should be null whenever the corresponding back electromotive force harmonics are null. Indeed, it doesn't produce useful average thrust. Finally, we verify with the *Rc*5 and *Ro*7 processors that:

$$i_{\alpha ref} \cdot \frac{d\tilde{\phi}_\alpha}{dx} + i_{\beta ref} \cdot \frac{d\tilde{\phi}_\beta}{dx} = T_{emREF} \qquad (3)$$

2.2 Controller design in (*α-β*) reference frame

As the currents i_α and i_β have a sinusoidal form in the steady-state, we need to use a controller that works with sinusoidal errors. That's what the resonant controllers are devoted to. In this way, the tracking of the reference currents and the rejection of disturbances from currents can be simultaneously realised. As previously explained, the resonant controllers are placed inside the *Rc*3 processor. The general transfer function of a resonant controller is given by:

$$C(s) = \frac{b_2 s^2 + b_1 s + b_0}{s^2 + \omega_0^2} \qquad (4)$$

Wherein b_0, b_1, b_2 denote the coefficients of associated resonant elements and ω_0 corresponds to the concerned resonant frequency.

The controller coefficients can be determined by using the pole assignment technique [8]: All poles of the closed-loop system are placed on a vertical line in the pole-zero map, as shown in Fig.3 [9]. Then, we choose $\Omega = \omega_0$ to control the system zeros around another vertical line, therefore minimizing their influences on system stability.

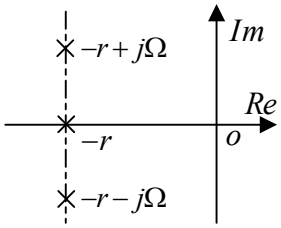

Fig.3: Pole assignment strategy

The speed control of synchronous motor implies that the speed, and so the current frequency, are variable. Thus, ω_0 and the coefficients b_0, b_1, b_2 need to be recalculated at each instant.

2.3 Control structure in (*d-q*) reference frame

If we apply the inversion principle on our PMLSM model, we obtain this controller design, Fig.4:

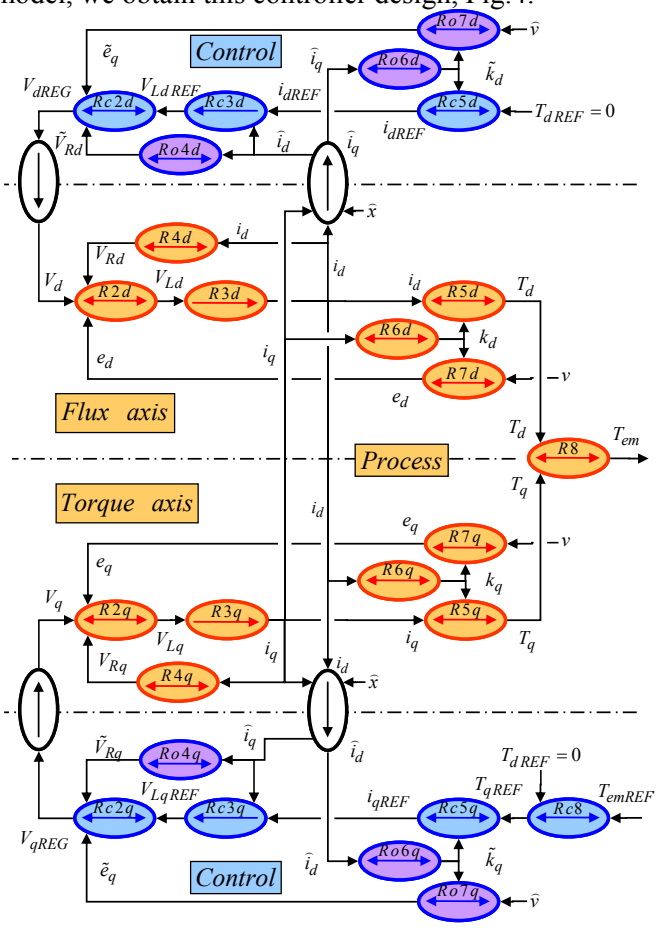

Fig.4: PMLSM thrust control scheme in (*d-q*)

The different relations are given by:

$$Rc2d \rightarrow V_{dREG} = V_{LdREF} - \tilde{V}_{Rd} - \tilde{e}_d$$

$$Rc2q \rightarrow V_{qREG} = V_{LqREF} - \tilde{V}_{Rq} + \tilde{e}_q$$

$$Rc3d \rightarrow V_{LdREF} = C_d(i_{dREF} - \hat{i}_d)$$

$$Rc3q \rightarrow V_{LqREF} = C_q(i_{qREF} - \hat{i}_q)$$

$$Ro4d \rightarrow \tilde{V}_{Rd} = \tilde{R}_d \cdot \hat{i}_d\,,\ Ro4q \rightarrow \tilde{V}_{Rq} = \tilde{R}_q \cdot \hat{i}_q$$

$$Rc5d \rightarrow i_{dref} = \frac{-T_{dREF}}{\tilde{k}_d},\ Rc5q \rightarrow i_{qref} = \frac{-T_{qREF}}{\tilde{k}_q}$$

$$Ro6d \rightarrow \tilde{k}_d = N_p \cdot \tilde{L}_q \cdot \hat{i}_q$$

$$Ro6q \rightarrow \tilde{k}_q = N_p \cdot (\tilde{L}_d \cdot \hat{i}_d + \sqrt{3/2} \cdot \tilde{\hat{\phi}}_f)$$

$$Ro7d \rightarrow \tilde{e}_d = \tilde{k}_d \cdot \hat{v}\,,\ Ro7q \rightarrow \tilde{e}_q = \tilde{k}_q \cdot \hat{v}$$

$$Rc8 \rightarrow T_{qREF} = T_{emREF} - T_{dREF}$$

The *Rc8* processor is called a strategy block, because we have several choices to generate the reference currents: the chosen reference currents should produce a linear control of the required thrust. In addition, reduction of ohmic losses induced by current i_d should be preferred [7]. According to the model with *Ro6d* and *Ro6q* processors (Fig.4), we can notice that the PMLSM can be decomposed into two DC motors. Consequently, in order to have a linear thrust control, we have chosen:

$$I_{dREF} = 0,\ \ Thus\ \ T_{dREF} = 0 \qquad (5)$$

The *Ro4* processor is defined to compensate the resistor voltage. The resistance value must be well known for this compensation to be perfect. But, as the resistance value depends on the resistance temperature induced by the current, it has finally been needed to have a precise temperature model of resistance variation. In fact, the P controllers of the current closed control loop are replaced by an IP controller (*Rc3d* and *Rc3q* processors). Indeed, at a steady state, the resistor voltage is constant, and the integral action will eliminate this constant error.

The *Ro7d* and *Ro7q* processors represent the back-EMF estimators. Yet, as we only discuss of the closed current loop here, the error on the thrust corrected by the EMF estimator is constant in the steady state (steady speed) [10]. So the correction error of this thrust error could be reported outside the current closed control loop to the speed control loop, by using an IP controller, which will be the focus of the next chapter. Then, the control structure is modified as presented in Fig.5.

We can notice that the fewer estimators a control structure needs, the more robust it will be. Indeed, robustness of a control structure depends on the high accuracy of estimators. The other extreme is the perfect modelling of all the studied systems. So it becomes possible to control the system with an open-loop control structure [11]. For adapted references, the control structure will feed the system with the fastest possible response, as no controller is needed. Nevertheless, the lack of robustness of such a control strategy is the main drawback.

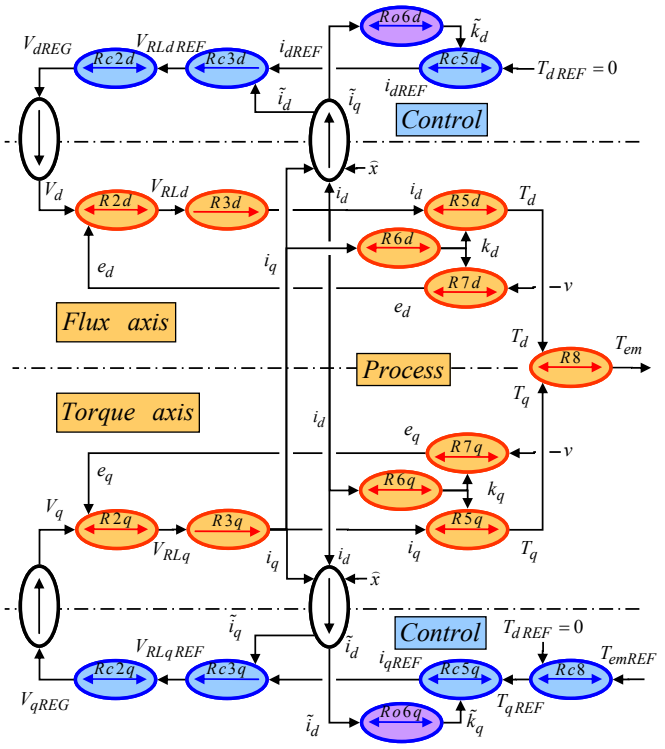

Fig.5: simplified PMLSM thrust control scheme

2.4 Controller design in (*d-q*) reference frame

The controllers in the *Rc5d* and *Rc5q* processors have to control the current closed loop. As in Park's reference frame, currents are constant at a steady state: a P controller is sufficient to eliminate the error. But, to take into account uncertainties and variations of the resistor value, the use of IP controllers improves the robustness of the current closed control loop:

$$C_d(s) = k_{cd} \cdot \left(1 + \frac{1}{\tau_{cd} \cdot s}\right), \quad and \quad C_q(s) = k_{cq} \cdot \left(1 + \frac{1}{\tau_{cq} \cdot s}\right) \qquad (6)$$

The integrator constant time is based on the constant time need by the closed current loop. Here in Fig.5, we notice that the current closed loop is defined by a first order with the *R3q* processor. Thus, the integrator constant time is equal to the electrical constant time:

$$\tau_{cd} = \tau_{cq} = \tilde{\tau}_e = \frac{\tilde{L}_q}{\tilde{R}_q} \qquad (7)$$

2.5 Experimental validation

The proposed approach has been experimentally verified on a laboratory test system equipped with a Rexroth LSP120C linear motor, Fig.6. Table 1 lists the specifications of the test system. The control scheme depicted in Fig.2 and Fig.4 has been implemented in a dSPACE DS1005 real-time digital control card to drive the PMLSM through an IGBT inverter. We have used a Heidenhain exposed linear encoder with a grating period of 20µm, which is a high precision incremental encoder, to detect the mover position.

Fig.6: Linear Motor Rexroth LSP120C

Table 1: The test system: specifications and parameters

Specifications		Parameter Value
PMLSM	Inductance	$L_s = 16.2[mH]$
	Resistance	$R_s = 1.1[\Omega]$
	Max value of magnet excitation flux / phase	$\hat{\phi}_f = 0.65[Wb]$
	Pole pitch	$\tau = 37.5[mm]$
	Electrical position constant	$N_p = 83.8[mm^{-1}]$
	Mass of mobile part	$M = 200[kg]$
Switching Frequency of IGBT		10 [*kHz*]

Fig. 7 presents the reference and estimated thrust. Furthermore, we can find reference and measured currents.

The currents shown in Fig.7 are defined in the (α-β) reference frame: we can notice that they are sinusoidal and are offset by $\pi/2$. The thrust generated has ripple force induced by the non-sinusoidal back electromotive force of the studied PMLSM.

We have used an AC current control system using one-frequency resonant controllers. In order to compensate the back electromotive force, we can use an AC current control system using two-frequency resonant controllers.

In the Fig.7 results, the load currents are very close to their references. The maximal delay of the load currents stays under 0.5ms, even if brutal changes occur in current references. When the non-sinusoidal Back-EMF is not compensated, we notice a ripple of 5% on thrust estimation.

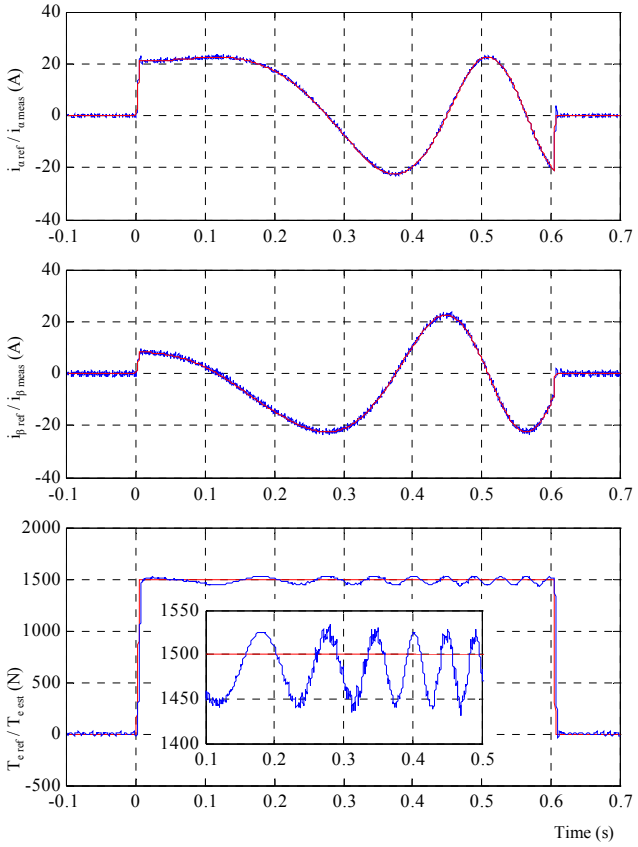

Fig.7: AC current control using resonant controllers

3 Speed control

3.1 Control structure

Fig.8 presents the speed control structure of a PMLSM with estimators:

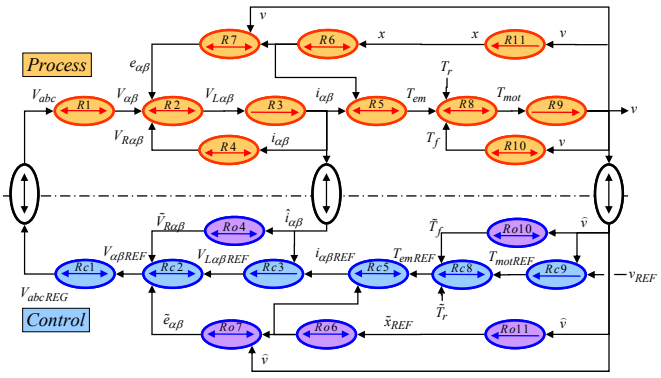

Fig.8: PMLSM speed control scheme with estimators

The *Ro*4, *Ro*7, *Ro*11, and *Ro*10 processors are considered as estimators because they use measurements. These processors are designed to compensate the resistor voltage drop, the back electromotive force and the friction phenomena.

The Fig. 9 presents the speed control structure of a PMLSM with anticipations:

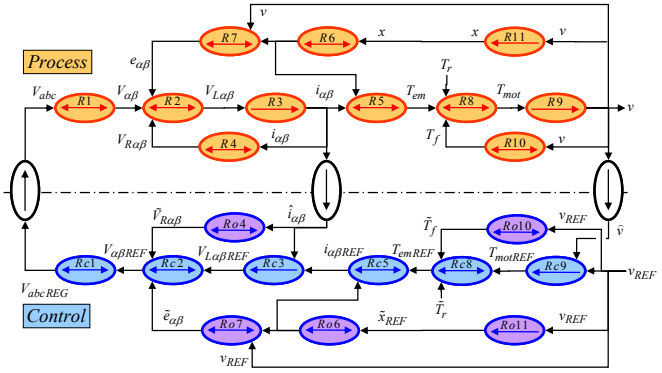

Fig.9: PMLSM speed control scheme with feedforward

The *Ro*7, *Ro*10 and *Ro*11 processors are directly fed by the speed reference. This design is called a feedforward supply. The aim is to compensate the back-electromotive force, the friction phenomena and to calculate the reference position. The main difference with the estimator structure is that the desired speed value is given instantly to the controller instead of the measured speed.

3.2 Controller design

The compensation of the friction phenomena is really difficult, because its model is too non-linear for a simple control strategy. Furthermore, even with an accurate model, it is difficult to have a robust controller. So, the classical solution is to use an IP controller inside the *Rc*9 processors. An example of controller design technique is based on the pole placement strategy [12].

4 Position control structure

Fig.10 presents the position control structure of a PMLSM with estimators:

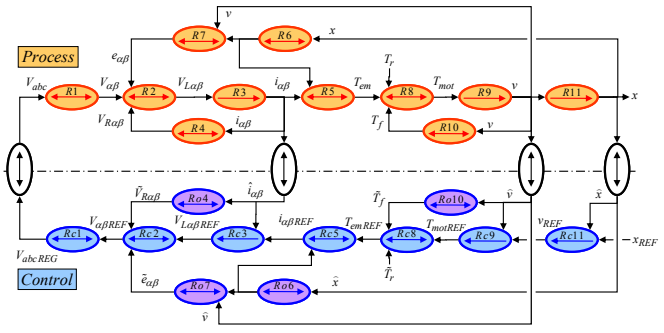

Fig.10: PMLSM position control scheme with estimators

The *Ro4*, *Ro7* and *Ro*10 processors are considered as estimators because they use measurements. These processors are designed to compensate the resistor voltage drop, the back electromotive force and the friction phenomena (same principle as in Fig.8).

Fig. 11 presents the position control structure of a PMLSM with a speed feedforward:

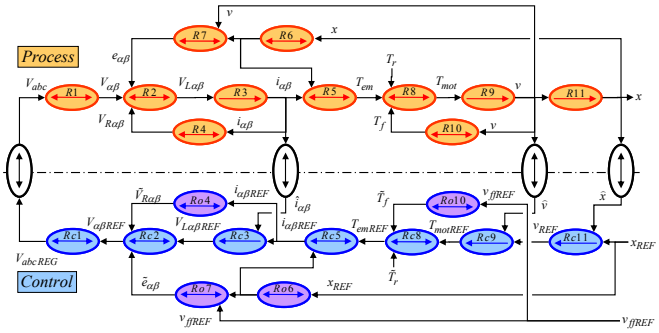

Fig.11: PMLSM position control scheme with a speed feedforward

The *Ro*7 and *Ro*10 processors are directly fed by the speed reference. This design is called a feedforward supply. The aim is to compensate the back-electromotive force and the friction phenomena. The difference with the principle of Fig.9 is that the position reference is directly calculated by the position generator [11].

5 Conclusion

In this paper, we have presented the control of synchronous motors. In Part I, we presented the model of a synchronous motor in several reference frames. We applied the Causal Ordering Graph (COG) formalism to PMSM and PMLSM models. Then, in this Part II, we have applied the inversion principle of the COG to design control structure in (α-β) reference frame and (d-q) reference frame. Several results show the interest of the Causal Ordering Graph for the design of control structure.

The next paper will focus on the PMLSM control structure, particularly on the comparison between the performances of industrial control structure and those of the different control structure presented in this paper. The controller design will have a special attention regarding to the possibility offered by the linear motor.

References:

[1] J.P. Caron, J.P. Hautier, *Modélisation et commande de la machine asynchrone*. Editions Technip, Paris, ISBN: 2-7108-0683-5, 1995 (In French).

[2] F. Blaschke, The principle of Field Orientation as applied to the new Transvector Closed Loop Control System for rotating field machine, *Revue Siemens*, Vol. 39, pp 11-13

[3] W. Leonhard, Adjustable-Speed AC drives, *Proceedings of the IEEE*, Vol.76, No.4, 1988, pp 455-471.

[4] P. Vas, *Sensorless Vector Control and direct Torque Control*, Oxford University Press, 1998.

[5] R. Becker, L. Still, AC propulsion system for Class 101-Requirements and solutions for high power drives, *In Symposium on AC Drives for Railway Applications*, Eindhoven University of Technology, December, 10th, 1996.

[6] J.P. Hautier, P.J. Barre, The Causal Ordering Graph A tool for system modelling and control law synthesis, *Journal of studies in informatics and control*, Vol.13, No.4, 2004, pp.265-283.

[7] D.C. Hanselman, Minimum torque ripple, maximum efficiency excitation of brushless permanent magnet motors, *IEEE Transactions on Industrial Electronics*, Vol.41, No.3, 1994, pp.292-300.

[8] J. Zeng, G. Remy, P. Degobert, P.J. Barre, Thrust Control of the Permanent Magnet Linear Synchronous Motor with Multi-Frequency Resonant Controllers, *in Proceedings of the 18th International Conference on Magnetically Levitated Systems and Linear Drives* (Maglev'2004), Shanghai, China, Vol.2, October 2004, pp.886-896.

[9] J. Zeng, P. Degobert, J.P. Hautier, Torque Ripple Minimization in Permanent Magnet Synchronous Motor Drives, *the 6th International Symposium on Advanced Electro Mechanical Motion Systems* (ELECTROMOTION 2005), Lausanne, Switzerland, 27-29 September 2005.

[10] G. Remy, J. Gomand, P.J. Barre, J.P. Hautier, New Current Control Loop with Resonant Controllers by using the Causal Ordering Graph - Application to Machine Tools, *WSEAS Transactions on Systems*, Vol.5, No.1, 2006, pp. 233-239.

[11] R. Béarée, J. Gomand, P.J. Barre, J.P. Hautier, Control structure synthesis based on the natural causality inversion, *WSEAS Transactions on Systems*, Vol.5, No.1, 2006, pp. 9-16.

[12] P.J. Barre, A. Tounzi, J.P. Hautier, S. Bouaroudj, Modelling and thrust control using resonating controller of asymmetrical PMLSM, *The 9th European Conference on Power Electronics and Applications*, EPE2001, Graz, 27-29 August, 2001.